Tellus (1988), *40B*, 380–392

The transformation of nitrogen oxides in the polluted troposphere

By C. S. ATHERTON and J. E. PENNER, *Lawrence Livermore National Laboratory, P.O. Box 808, Livermore, CA 94550, USA*

(Manuscript received 2 November 1987; in final form 18 March 1988)

ABSTRACT

The transformation of nitrogen oxide was investigated using an explicit chemical reaction mechanism developed for use in tropospheric photochemical models. Through box-model simulations, the mechanism was first used to study the formation of organic nitrate species in an urban setting for a range of hydrocarbon to NO_x ratios. Next, several changes to the basic mechanism were incorporated to study their effect on organic nitrate formation. The results show organic nitrates are present and their amounts depend on the ratio of hydrocarbons to NO_x. At high HC/NO_x ratios, as much as 24% of the nitrogen emitted into an urban area may be transformed to organic nitrates. Experimental evidence on the yields and rates of some reactions is scarce.

1. Introduction

Nitrogen oxides play an important role in tropospheric chemistry. In "clean" continental areas, nitrogen oxides act to form ozone via the reaction sequence:

$$HO_2 + NO \rightarrow HO + NO_2 \quad (1)$$

$$NO_2 + h\nu \rightarrow NO + O \quad (2)$$

$$O + O_2 + M \rightarrow O_3 + M. \quad (3)$$

Nitrogen oxide transformation is also important because nitrogen oxides, in the form of NO_2, combine with hydroxyl to form nitric acid, a significant component of "acid rain":

$$HO + NO_2 + M \rightarrow HNO_3 + M \quad (4)$$

Reaction (4) also serves to suppress O_3 formation in the more highly urbanized areas and in areas of low HC/NO_x. In these areas, reaction (4) may dominate the removal of HO_x. Since HO_x is necessary to initiate the photochemical oxidation of hydrocarbons that leads to smog, the removal of HO_x slows O_3 formation. In these areas, nitrogen oxides which are primarily emitted as NO also remove O_3 directly via:

$$NO + O_3 \rightarrow NO_2 + O_2 \quad (5)$$

This reaction leads to a net reduction in O_3 until a steady state ratio for NO/NO_2 is established by reactions (2), (3), and (5).

A large fraction of the reactive nitrogen present in the troposphere is emitted as NO_x from fossil fuel burning (Logan, 1983), an activity which occurs primarily in urban areas. In the past, photochemical models have generally assumed that most of this NO_x was then converted to either NO, NO_2, HNO_3, PAN ($CH_3C(O)O_2NO_2$) or particulate nitrate (NO_3^-). However, recent measurements have indicated that a significant portion of the total reactive odd nitrogen reservoir at a variety of locations is not accounted for by the sum of these five species (Fahey et al., 1986; Singh, 1987; Parrish et al., 1986). Thus, it is important to examine in detail whether nitrogen oxide transformations in an urban environment can lead to species other than the five above and if they represent a significant fraction of the reactive nitrogen reservoir.

To examine this question in detail, as well as the effects of uncertainties in chemical mechanisms, requires the use of a fully explicit photochemical model. In general, though, most

urban smog models, as well as regional oxidant models, only treat chemistry in a "lumped" or "condensed" fashion. This is necessary because large grid-based models cannot possibly treat in detail the large number of hydrocarbon species generally found within an urban environment. The condensed models are often validated by their ability to predict ozone and thus, may not be appropriate for use in examining details of nitrogen chemistry. We, therefore, used an explicit chemical mechanism in box model simulations to investigate the formation of organic nitrate species.

In Section 2, we describe the explicit chemical mechanism used in this work. Urban scale nitrogen transformation is examined using a photochemical box model which is described in Section 3. The conditions tested are described in Section 4 and our results appear in Section 5. We show that for high hydrocarbon to NO_x ratios, as much as 24% of the reactive nitrogen reservoir can be transformed into organic nitrate species. We also examine the effects of several changes to the basic photochemical mechanism. These changes, suggested by Fahey et al. (1986) and Singh (1987), do not lead to significant enhancement of the organic nitrate reservoir for our conditions. Finally, we examine the representative nitrogen species used in a typical condensed mechanism to those of the explicit model. Significant differences are found, particularly when the chemistry of the explicit mechanism for PAN analogues is considered.

Table 1. *Hydrocarbon species present in the explicit chemical reaction mechanism*

propane
n-butane
isobutane
n-pentane
n-hexane
n-heptane
n-octane
n-nonane
2-methylpentane
2,3-dimethylbutane
2,4-dimethylpentane
2,2,4-trimethylpentane
ethene
propene
isobutene
1-butene
trans-2-butene
toluene
benzene
m-xylene
o-xylene
1,3,5-trimethylbenzene
formaldehyde
acetaldehyde
propionaldehyde
glycolaldehyde
benzaldehyde
methyl ethyl ketone
methyl glyoxal
acetone
glyoxal
biacetyl
nitrophenol
cresol
phenol

2. Chemical mechanism

The transformation of nitrogen species was investigated using an explicit chemical reaction mechanism in a box model approach. The explicit mechanism (Carter et al., 1986) contains over 450 reactions and 170 species. The hydrocarbon species we modeled are shown in Table 1. In our simulations, we included 12 alkanes, 5 alkenes, 5 aromatics, and 5 aldehydes. The reaction of each hydrocarbon with OH results in the creation of a distinct peroxy radical. The total peroxy and peroxyacyl radical concentrations are kept track via the counter pseudo-species RO_2 and RCO_3, respectively. Radical-radical reactions are not represented explicitly, but somewhat semi-explicitly: a specific radical reacts with the total peroxy radical concentration, RO_2, or total peroxyacyl radical, RCO_3, rather than with each of the other radicals separately. Specific radicals also react with NO and HO_2.

3. Box-model simulations

The explicit mechanism was incorporated into a box model. The box model used for the simulations solves the species continuity equation:

$$\frac{\partial C_i}{\partial t} = R_i + \frac{S_i}{H} - \frac{1}{H}\frac{\partial H}{\partial t}(C_i - C_{i,0}), \qquad (6)$$

where C_i = concentration of chemical species i, H = average mixed layer depth, S_i = average source flux for species C_i, R_i = chemical reaction rate terms for production and consumption of species i, and $C_{i,0}$ = concentration above mixed layer of species i, taken to be 0.

Several of the parameters required for the box model were taken from calculations performed for a 25 × 25 km region in the San Francisco Bay Area by the Livermore Regional Air Quality Model (LIRAQ) (Penner, 1984; Penner and Connell, 1987). This model is a three dimensional photochemical transport model. Its 200 × 200 km domain allows for modeling the fate of chemicals in the San Francisco region. The average mixed-layer depth, H, was set at 300 m, and $1/H\ (\partial H/\partial t)$, was set equal to 2.4×10^{-5} s^{-1}. Photolysis rate constants were set equal to those for a 45° zenith angle, and were held constant for 8 h, the length of the simulation. The temperature was 298°K. (Simulations conducted at a lower temperature of 291°K did not differ significantly from those for 298°K). For the simulations described in this paper, there were no sources of pollutants during the run.

Box models are often used to simulate laboratory smog chamber experiments. In these laboratory settings, the chamber itself may be a source of radicals, and this phenomenon must be taken into account by including appropriate "wall reactions" in the chemical mechanism. Because we were interested in the ability of these mechanisms to simulate atmospheric conditions, however, we did not include any chamber dependent reactions in the models.

4. Initial conditions

Three sets of initial conditions, having HC/NO_x ratios (ppbC/ppb NO_x) of 2, 7, and 28, were simulated. These are modifications of the initial conditions used by Leone and Seinfeld (1985), and cover an important range of HC/NO_x for tropospheric modeling. The HC/NO_x = 7 set was loosely based on SAPRC smog chamber experiment SUR-119J (see Leone and Seinfeld, 1985). The HC/NO_x = 2 conditions were determined by halving the total hydrocarbon concentration and doubling the NO_x concentration of the HC/NO_x = 7 set. Correspondingly, the HC/NO_x = 28 conditions were calculated by doubling the hydrocarbon concentration, and halving the NO_x concentration of the HC/NO_x = 7 set.

Using these total hydrocarbon and NO_x concentrations, we initialized individual hydrocarbon species as follows. Note the initial conditions for HC/NO_x = 7 are shown in Table 2. The total hydrocarbon concentration given by Leone and Seinfeld (1985) was first converted to ppbC and

Table 2. *Initial concentrations for HC/NO_x = 7*

Species	Concentration (molecules cm^{-3})
propane	2.18 (12)*
n-butane	1.14 (12)
isobutane	6.03 (11)
n-pentane	5.48 (11)
n-hexane	8.02 (11)
n-heptane	1.79 (11)
n-octane	5.73 (10)
n-nonane	6.01 (10)
2-methylpentane	6.87 (11)
2,3-dimethylbutane	2.35 (11)
2,4-dimethylpentane	1.97 (11)
2,2,4-trimethylpentane	2.24 (11)
ethene	9.26 (11)
propene	9.81 (11)
isobutene	2.78 (11)
1-butene	1.90 (11)
trans-2-butene	3.39 (11)
toluene	1.41 (12)
benzene	4.60 (11)
m-xylene	3.29 (11)
o-xylene	1.34 (11)
1,3,5-trimethylbenzene	2.74 (11)
formaldehyde	1.85 (12)
acetaldehyde	6.17 (11)
NO	7.38 (12)
NO_2	1.23 (12)
HONO	2.95 (11)
CO	1.83 (14)
H_2O	2.14 (17)
O_2	5.17 (18)
M	2.46 (19)
total RHC, (atoms C cm^{-3})	5.74 (13)
total NO_x (molecules cm^{-3})	8.61 (12)

*Note: 2.18 (12) ≡ 2.18×10^{12}.

summed. This sum was then partitioned into eleven hydrocarbon categories using the recommended default hydrocarbon split for surface species (Lurmann et al., 1987), shown in Table 3. Our HC/NO_x values are slightly lower than previous simulations (Leone and Seinfeld, 1985) because the recommended split includes a small percentage of unreactive hydrocarbons, whose concentrations are not simulated in the chemical mechanism.

Next, specific hydrocarbon concentrations within each of the eleven categories were set using the results of sampling conducted in the Bay Area (Koppe, 1981). Specifically, the sampling results of 0600–0700 on September 30, 1980 in San Jose were used. The relative contribution of each hydrocarbon to the total category concentration was assumed to be equal to its measured concentration (in ppbC) divided by the total concentration observed for the category (also in ppbC). This fraction was then multiplied by the category concentration determined by the recommended default split. Finally, concentrations in ppbC were converted to molecules cm^{-3}. In this way, the concentrations for the explicit mechanism shown in Table 2 were set.

The total reactive hydrocarbon concentrations used, 1170, 2335, and 4670 ppbC are similar to those that might be expected for a polluted urban area. Hydrocarbon levels of 1500–3000 ppbC have been measured in the San Francisco area between 0500 and 0800 (Koppe, 1981). A range of measurements have also been made in the Los Angeles area (Grosjean and Fung, 1984). The values selected from this range for other work (Calvert and Madronich, 1987) yielded 1900 pbbC NMHC. The hydrocarbon concentrations we used are somewhat higher than for cities not located in California. A survey of seven such U.S. cities reported mean nonmethane hydrocarbon concentrations of 1360, 580, 560, 570, 580, 370, and 230 ppbC (Sexton and Westberg, 1984) and measurements in a semi-rural area in West Germany yielded hydrocarbon levels of 150 ppbC (Rudolph and Khedim, 1985).

Table 3. *Recommended default NMOC composition profiles* for surface layer non-methane organic carbon*

Compound	Carbon fraction of NMOC
C4-C5 alkanes	0.21
C6+ alkanes	0.28
ethene	0.03
terminal alkenes	0.06
internal alkenes	0.04
mono-alkylbenzenes	0.16
di-alkyl benzenes	0.06
tri-alkyl benzenes	0.04
formaldehyde	0.03
acetaldehyde	0.02
unreactive	0.07

*Taken from Lurmann et al. (1987).

5. Results and discussion

5.1. Base case

The results of an 8-h base case run of the explicit mechanism for the three HC/NO_x ratios are shown in Fig. 1. They are plotted in terms of the quantity X/NO_y, which is defined as $X/NO_y = 1 - [\sum (NO + NO_2 + NO_3^- + PAN + HNO_3)/NO_y]$. NO_y denotes total reactive odd nitrogen = $NO + NO_2 + NO_3^- + PAN + HNO_3 + 2N_2O_5 + \ldots$ In the past, the species NO, NO_2, NO_3^-, PAN, and HNO_3 were assumed to account for the bulk of the total reactive nitrogen reservoir. The quantity X/NO_y, then denotes the fraction of total odd reactive nitrogen present as species other than the five listed above. Because our reaction mechanism is gas phase only, in our simulations $[NO_3^-] = 0$.

As shown in Fig. 1, the most dramatic increase in X/NO_y occurs for $HC/NO_x = 28$. The explicit mechanism predicts a maximum X/NO_y of 0.24. Similarly, for $HC/NO_x = 7$, the explicit mechanism predicts an X/NO_y of 0.09. At $HC/NO_x = 2$, the quantity X/NO_y is so small it is not significantly different from zero.

It can be seen in Fig. 1 that the quantity X/NO_y rises rapidly for the first 3 h for $HC/NO_x = 28$, and then increases only slightly as time increases. For the $HC/NO_x = 2$ and 7 cases, however, even after 8 h, the fraction X/NO_y is still increasing and has yet to reach a maximum. Even after much longer times, however, these two cases will not produce as high a level of X/NO_y as the $HC/NO_x = 28$ scenario. Below, we use the results of a 36-h simulation consisting of 12 h daylight, 12 h night, and 12 h daylight, respectively, to explain.

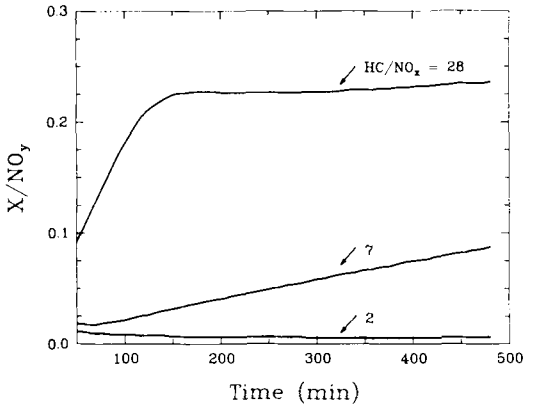

Fig. 1. Results of an 8-h base case simulation using the explicit mechanism for $HC/NO_x = 2$, 7, and 28. $X/NO_y = 1 - \{\sum([NO] + [NO_2] + [NO_3^-] + [PAN] + [HNO_3])/NO_y\}$.

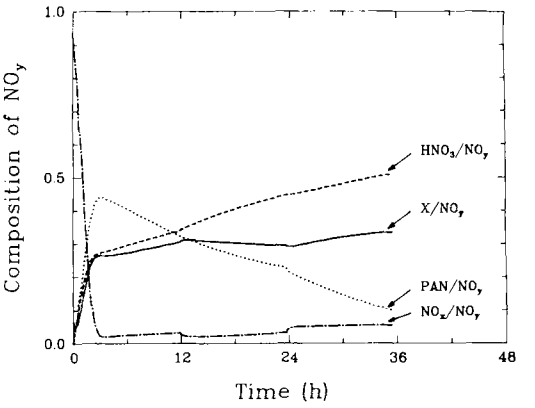

Fig. 2. Results of a 36-h simulation for $HC/NO_x = 28$. Daytime photolysis conditions occurred during 0-12 h and 24-36 h.

The fact that the amount and timing of the peak for X/NO_y depend on HC/NO_x can be seen in Figs. 2 and 3. These two figures show what fraction of nitrogen is present as NO_x ($NO + NO_2$), HNO_3, PAN, and the collective species comprising X/NO_y as a function of time for $HC/NO_x = 28$ and 7, respectively.

Consider the $HC/NO_x = 28$ case. Initially, over 90% of the nitrogen is present as NO_x. After only 3 h, however, essentially all of the NO_x has been transformed into other species, and NO_x/NO_y equals only 0.02. The nitrogen is present in the following fractions: $PAN/NO_y = 0.44$; $HNO_3/NO_y = 0.27$; and $X/NO_y = 0.27$.

The formation of HNO_3 and PAN is important because in the early stages, two of the most important routes of nitrogen transformation are:

$$NO_2 + OH \rightarrow HNO_3 \quad k = 1.00 \times 10^{-11} \tag{7}$$

$$CH_3CO\text{-}O_2 + NO_2 \rightarrow PAN \quad k = 2.8 \times 10^{-12} \times \exp(180/T). \tag{8}$$

The major paths of destruction for each of these species is:

$$HNO_3 + OH \rightarrow NO_3 + H_2O \quad k = 9.4 \times 10^{-15} \times \exp(778/T) \tag{9}$$

$$PAN \rightarrow CH_3CO\text{-}O_2 + NO_2 \quad k = 2.0 \times 10^{16} \times \exp(-13540/T) \tag{10}$$

During the first day, the destruction of HNO_3 is generally negligible compared to its production

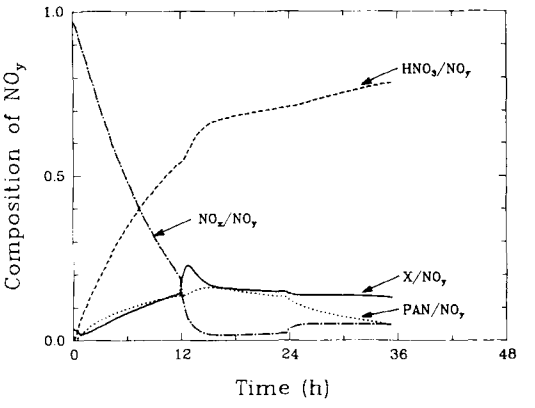

Fig. 3. Results of a 36-h simulation for $HC/NO_x = 7$. Daytime photolysis conditions occurred during 0-12 h and 24-36 h.

rate, but both the production and dissociation rates of PAN can be important.

Initially, when NO_2 is abundant, and the dilution of species (due primarily to inversion height movement) isn't appreciable, a net production of HNO_3 and PAN occurs. The initial production rates are approximately:

$$\frac{d[HNO_3]}{dt} = k_7[NO_2][OH] \tag{11}$$

$$\frac{d[PAN]}{dt} = k_8[CH_3CO\text{-}O_2][NO_2] \tag{12}$$

At high HC/NO_x, hydrocarbons are present in relatively high concentrations, as is the radical CH_3CO-O_2 which is produced by reactions of hydrocarbons. The OH concentration is lowered as it reacts with hydrocarbons and their products. For $HC/NO_x = 28$, $k_8[CH_3CO-O_2] \gg k_7[OH]$, so PAN is formed at a higher rate than HNO_3 initially.

Once all of the initial NO_x has been transformed to other species, the decomposition of PAN allows nitrogen to continue to be transformed into HNO_3, as well as nitrate species which constitute X/NO_y. For example, for $HC/NO_x = 28$, from time = 3 h to 12 h, PAN/NO_y decreases from 0.44 to 0.32; HNO_3/NO_y increases from 0.27 to 0.34; and X/NO_y increases from 0.27 to 0.31. The quantity NO_x/NO_y increases only slightly from 0.02 to 0.03. As can be seen in Fig. 2, the fraction HNO_3/NO_y is increasing faster than X/NO_y, so a greater fraction of the nitrogen liberated from PAN is transformed into HNO_3 than into any other species.

During the nighttime (12–24 h), PAN/NO_y continues to decrease, while HNO_3/NO_y steadily increases. The fraction X/NO_y increases slightly at time = 12 h due to the formation of NO_3 and N_2O_5, but then decreases mainly to the net decomposition of PAN analogues.

Once the sun rises (time = 24 h), an appreciable amount of nitrogen is still present as PAN ($PAN/NO_y = 0.23$). The fractions $HNO_3/NO_y = 0.45$, and $X/NO_y = 0.29$. Then, again, as in the first day, both HNO_3/NO_y and X/NO_y continue to increase as the decomposition of PAN releases nitrogen to the reactive cycle, but the relative rate of increase of HNO_3 is much faster.

Fig. 3 shows that for $HC/NO_x = 7$, the initial transformation of NO_x into other species takes much longer than 3 h. This is because the proportion of hydrocarbons to NO_x is much lower than for the $HC/NO_x = 28$ scenario. Thus, the concentration of CH_3CO-O_2, which is generated from hydrocarbons and produces PAN, is relatively lower than for $HC/NO_x = 28$. As well, the concentration of OH is relatively higher because there are fewer hydrocarbons with which it can react. Consequently, for $HC/NO_x = 7$, more HNO_3 and less PAN is formed initially than for $HC/NO_x = 28$. Since the reaction rate of HNO_3 with OH and its photolysis is negligible compared to the formation of HNO_3, once HNO_3 is formed, it effectively takes nitrogen out of circulation.

For the $HC/NO_x = 7$ scenario, at time = 12 h, $HNO_3/NO_y = 0.54$, indicating well over half the nitrogen has already been converted to HNO_3. The fraction X/NO_y only equals 0.14, $PAN/NO_y = 0.13$, and $NO_x/NO_y = 0.19$. During the early part of the night, between time = 12 and 15 h, the fraction NO_x/NO_y decreases from 0.19 to 0.02, indicating essentially all of the original nitrogen has been transformed to other species. During this same time, PAN/NO_y increases from 0.13 to 0.16. X/NO_y increases from 0.14 to a peak of 0.23, mainly due to the presence of NO_3 and N_2O_5, and HNO_3/NO_y increases from 0.54 to 0.66. After 15 h, the NO_3 and N_2O_5 concentrations are negligible, and X/NO_y begins to decrease. So, for the $HC/NO_x = 7$ case, the relative concentration of PAN once all of the initial NO_x has been transformed is much lower than for the $HC/NO_x = 28$ scenario (0.16 versus 0.44).

During the next daylight sequence (time = 24 to 36 h), the fraction PAN/NO_y decreases from 0.13 to 0.04, HNO_3/NO_y increases from 0.71 to 0.78, X/NO_y decreases from 0.14 to 0.13 and NO_x/NO_y increases from 0.02 to 0.05. Then, throughout the day, for the $HC/NO_x = 7$ case, virtually all of the nitrogen is then further transformed into HNO_3, so the fraction X/NO_y never is greater than its earlier peak amount of 0.14.

These effects are even further amplified for $HC/NO_x = 2$. So essentially, at the lower HC/NO_x ratios, much of the nitrogen is quickly transformed into HNO_3, which effectively removes it from the reactive cycle. Much less is initially transformed into PAN which, once all the initial NO_x is transformed, decomposes, allowing NO_x to return to the nitrogen cycle. Consequently, there is less nitrogen available to form other species (such as those that compose X/NO_y), and the fraction X/NO_y will be lower once all of the initial NO_x has reacted for lower HC/NO_x.

To understand which species are contributing to X/NO_y, the quantity X/NO_y was examined in greater detail. Fig. 4 shows the species which constitute significant fractions of X/NO_y for the explicit mechanism at $HC/NO_x = 28$. The explicit mechanism predicts the fraction of nitrogen

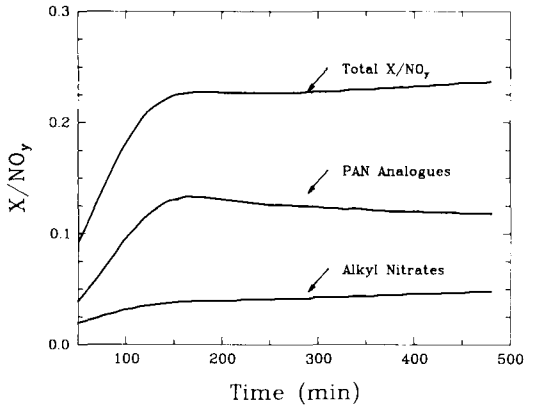

Fig. 4. Composition of X/NO_y for an 8-h base case simulation for $HC/NO_x = 28$.

present as alkyl nitrates as 0.05. The group entitled PAN Analogues accounts for the majority of X/NO_y for the explicit mechanism. These are further separated and compared to PAN in Table 4. The largest component is shown to be PPN, while smaller amounts of eight different PAN analogues are predicted.

The PAN analogues represent nitrogen compounds which result from the reactions of higher (C > 2) aldehydes and aromatic ring oxidation compounds. The chemical structure of the PAN analogues hasn't been fully determined, so what they represent is a nitrogen sink necessary for models of aromatic hydrocarbons to correctly predict ozone. They, therefore, contribute to X/NO_y. There are still many uncertainties concerning the true rate constants and yields for specific reactions (Carter et al., 1986). In the explicit mechanism, the reaction rates for the PAN analogues have been set equal to those of PAN, and their yields have been fit to satisfy experimental smog chamber data.

Table 4. *Relative concentrations of PAN-analogues after 8 hour simulation* ($HC/NO_x = 28$)

Species	% of X/NO_y	% of PAN
PPN	6.6	16.5
glyoxal-PAN	1.2	2.9
glycolaldehyde-PAN	0.6	1.6
benzene-PAN	0.4	1.0
benzaldehyde-PAN	0.2	0.4
toluene-PAN	1.2	3.0
m-xylene-PAN	0.5	1.3
o-xylene-PAN	0.2	0.4
trimethylbenzene-PAN	0.7	1.7
total	11.6	28.8

Consider the PAN analogues which arise from the reaction of aromatics with the hydroxyl radical (the only reaction of consequence for the aromatics) (Takagi et al., 1981; Hoshino et al., 1978). Aromatic reactions can occur via either hydrogen abstraction from a substituted alkyl group or OH addition to the ring structure. A small fraction (3–19%) of the aromatics react via the hydrogen abstraction pathway. The subsequent chemistry is fairly well understood and involves the formation of aromatic aldehydes and a small amount of benzyl nitrates (Hoshino et al., 1978; Tuazon et al., 1986; Gery et al., 1987). The explicit mechanism utilized here ignores this benzyl nitrate formation because it is so small. Until recently, only scarce data was available on the yields of these nitrates (Hoshino et al., 1978), but they may account for approximately 7–10% of the hydrogen abstraction pathway for xylenes (Gery et al., 1987).

The pathway of OH-addition, which leads to PAN analogue formation, is not as thoroughly understood. The OH-aromatic adducts initially formed react further to yield phenols, nitrophenols, and nitroarenes (Hoshino et al., 1978; Gery et al., 1987). Additionally, cleavage of the ring structure occurs, resulting in dicarbonyls such as glyoxal, methylglyoxal, biacetyl, and other unknown ring opening compounds. In the explicit mechanism, it is assumed that these unknown ring opening compounds lead to the formation of PAN analogues, although other degradation pathways that lead to similar nitrogen-containing species are perhaps also possible. The fraction of aromatics that undergo ring cleavage, and the subsequent products formed, are fairly uncertain (Carter et al., 1986) and are still being characterized for compounds ranging from benzene and toluene to trimethylbenzenes (Tuazon et al., 1986; Gery et al., 1987). Carbon balances indicate that all of the original aromatic carbon may still not be accounted for by all of the above processes (Tuazon et al., 1986).

Because the chemistry which leads to the formation of PAN analogues is so poorly

characterized, we cannot conclude that a significant portion of the reactive nitrogen reservoir should be in this form. However, the conversion of reactive nitrogen in the form of NO and NO_2 to a less reactive form such as a PAN analogue is required in order for the explicit model to accurately predict ozone formation (Carter et al., 1986). Similar agreement could result if the aromatic ring opening compounds lead to other nitrate forms. In particular, the PAN analogues themselves may form as assumed here, but degrade via autodissociation (analogous to PAN itself) to form other nitrates (see discussion below).

5.2. Mechanisms of organic nitrate formation

Appreciable values of X/NO_y have been measured for certain locations. At Niwot Ridge, for example, measurements of NO, NO_2, HNO_3, NO_3^-, PAN, and total reactive nitrogen (NO_y) showed that these individual species only accounted for 55% of the total reactive nitrogen in the summer, and 88% in the fall (Fahey et al., 1986). In other words, X/NO_y was equal to 0.45 in the summer, and 0.12 in the fall. Similar measurements made in marine air near the coast of California yielded an X/NO_y of 0.25 (Singh, 1987). The measurements are of interest because much of the nitrogen present in rural areas may have been transported from an urban area and experienced urban levels of hydrocarbons and NO_x. At rural locations, though, the anthropogenic hydrocarbon and NO_x concentrations are lower than we simulated, and natural hydrocarbons and NO_x may play a role in the nitrogen shortfall. Thus, our simulations do not directly apply to the measurement sites.

Following these measurements, several hypotheses concerning the formation of organic nitrate species were postulated (Fahey, et al., 1986; Singh, 1987). We next performed calculations to see if these mechanisms could impact the organic nitrate levels of air parcels that have been exposed to urban levels of anthropogenic pollution.

First, the fraction of alkyl nitrates composing X/NO_y may be increased if the fraction of C_6+ alkanes present in the initial split of hydrocarbons is altered. C_6+ alkanes degrade to form organic peroxy radicals that react with NO to form alkyl nitrates. Calvert and Madronich (1987) suggested that as much as 21% of the original hydrocarbon mixture might degrade to form alkyl nitrates under high NO_x conditions.

A second mechanism, the autodissociation of PAN to form methyl nitrate (Singh, 1987; Stephens, 1969), may result in an increase of the organic nitrate fraction of X/NO_y and in a nitrogen species previously disregarded.

A third potential source of nitrates that was neglected in our base case is from the oxidation of naturally occurring hydrocarbons such as the terpenes. These biogenic emissions may contribute significantly to the total hydrocarbon concentration. Products of isoprene oxidation, for example, include nitrate species (Lloyd et al., 1983).

Finally, the possibility that an aerosol is responsible for the discrepancy in the nitrogen measurements has been raised (Fahey et al., 1986). We test the effects of the first three hypotheses here.

We first investigated how organic nitrates produced from the reaction of peroxy radicals and NO affect X/NO_y. The explicit mechanism already produces organic nitrates from the reaction of alkyl peroxy radicals and NO. In the literature, alkyl nitrate formation has been studied mainly for the alkanes. The rate for the reaction:

$$RO_2 + NO \rightarrow products \qquad (13)$$

has been measured for $R = CH_3$ (for example, see Cox and Tyndall, 1979) and C_2H_5. Atkinson and Lloyd (1984) summarized the results of sixteen such efforts. Their recommendation was an overall rate constant of $4.2 \times 10^{-12} \times \exp(180/T)$ for all RO_2 radical reactions with NO, which is used in the explicit mechanism. Reaction (13) occurs via two different pathways:

$$RO_2 + NO \rightarrow RO + NO_2 \qquad (13a)$$

$$RO_2 + NO \rightarrow RNO_3 \qquad (13b)$$

Studies have shown (Darnall et al., 1976; Atkinson et al., 1982a; Atkinson et al., 1983; Atkinson et al., 1984; Atkinson, et al., 1987) that as the carbon number of species R increases, the ratio $k_b/(k_a + k_b)$ also increases. Thus, longer chain alkanes produce a higher fraction of alkyl nitrates than do the shorter chains. The value of $k_b/(k_a + k_b)$ for straight chain alkanes ranges from

≤ 0.014 for ethane to 0.318 ± 0.027 for *n*-octane (Atkinson et al., 1982a). Also, the value of $k_b/(k_a + k_b)$ increases as the amount of branching in the alkane increases (Atkinson et al., 1984). These rate constants have been shown to be pressure and temperature dependent (Atkinson et al., 1983; Atkinson et al., 1987).

In the explicit mechanism, the organic nitrates formed are not represented exactly but in terms of two representative nitrates: 2-butyl and 4-heptyl nitrate. The fractional yield of organic nitrates formed, however, does depend on the number of carbons present in the parent alkane.

The first calculation was made to see the effect longer chain alkanes have on the amount of alkyl nitrates formed. We simulated how organic nitrate concentrations would change if the initial air parcel composition was assumed to be exclusively $\geq C_6$ alkanes. Since the higher carbon number alkanes should produce higher yields of alkyl nitrates, by maximizing the number of C_6+ alkanes, we should increase the alkyl nitrate concentration.

The second hypotheses tested was methyl nitrate formation from the autodissociation of PAN (Singh, 1987). PAN is ubiquitous, and may reach concentrations of 0–100 ppbv in the polluted atmosphere and 10–100 pptv in the remote atmosphere (Singh and Salas, 1983). PAN may also be transported long distances (Hov, 1984). If PAN forms other nitrate species, they may be present in high enough quantities to significantly alter the composition of the reactive odd nitrogen reservoir. Also, as discussed above, the PAN analogues could be an appreciable source of alkyl nitrates if they degrade in a similar fashion to form alkyl nitrates.

The unimolecular decomposition of PAN was hypothesized by Stephens (1969), who observed that a decrease in PAN concentrations in a storage tank was matched by increases in methyl nitrate and carbon dioxide concentrations, in approximately equimolar amounts. He postulated PAN formed a cyclical intermediate which then decayed to form methyl nitrate. Recent experimental results (Senum et al., 1986) indicate that two pathways of PAN decomposition are possible, one being the proposed cyclical autodissociation. Assuming the reaction proceeds homogeneously, the reaction rate for this cyclical transition state decomposition was measured to be $2.1 \times 10^{12} \times \exp[(-24800 \pm 1800)/RT]$ s^{-1} (Senum et al., 1986). We used the value $2.1 \times 10^{12} \times \exp[-12480/T]$ s^{-1} for the rate constant. If this reaction is shown to be heterogeneous, it could still be important in areas with appreciable particulate concentrations.

It was necessary to incorporate the photolysis of methyl nitrate in the model. This rate has been measured to be 2.2×10^{-6} s^{-1} assuming solar flux intensities for a zenith angle of 45° and a quantum yield of 1 (Taylor et al., 1980). Methyl nitrate also reacts with the hydroxyl radical. The rate was recently measured to be $3.4 \pm 0.4 \times 10^{-14}$ cm^3 molecule^{-1} s^{-1} at 298°K (Gaffney et al., 1986). This reaction was not included since its lifetime due to photolysis is estimated to be much shorter than its lifetime due to reaction with OH. In simulations with a condensed model (Lurmann et al., 1987), the rate of loss of methyl nitrate due to photolysis was always slower than the rate of reaction with OH by a factor of 25–100.

Finally, the third hypothesis, involving nitrate formation from radicals formed during the oxidation of isoprene, was included in the model. It is possible that radical species created from these hydrocarbons may form appreciable amounts of organic nitrate species by reacting with NO or other nitrogen species. Given high enough natural fluxes, these nitrates could change the balance of the nitrogen reservoir. In order to estimate the effect of these naturally occurring hydrocarbons on organic nitrate concentrations, an isoprene reaction mechanism (Lloyd et al., 1983) was also included in the explicit mechanism. An initial isoprene concentration of 2.46×10^{10} molecules cm^{-3}, along with a flux rate of 2.0×10^{11} cm^{-2} s^{-1} was used, similar to average rates as estimated for the San Francisco Bay Area (Penner, 1984).

The results of these three scenarios, along with the base case, are presented in Figs. 5 and 6 for $HC/NO_x = 28$ and 7, respectively. The results for $HC/NO_x = 2$ do not differ for any scenario from those shown in Fig. 1, and are not pictured. For both $HC/NO_x = 7$ and 28, the greatest increase in X/NO_y occurs for the scenario in which the air parcel is assumed to initially contain alkanes with six or more carbon atoms. The quantity X/NO_y increases from 0.09 to 0.10 for $HC/NO_x = 7$, and increases from 0.24 to 0.26 for $HC/NO_x = 28$.

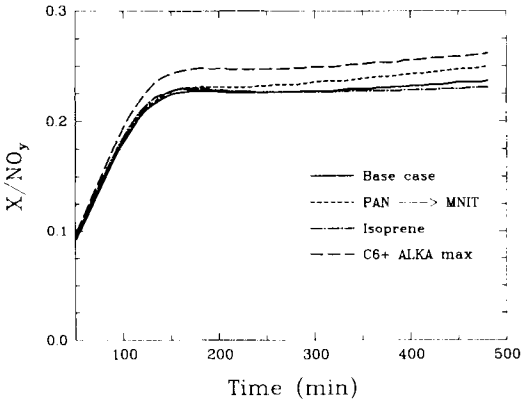

Fig. 5. X/NO_y as a function of time for four scenarios: the base case, a case including the unimolecular decomposition of PAN to form methyl nitrate, a case including an isoprene mechanism, and a case modeling an air parcel containing only $C \geq 6$ alkanes. $HC/NO_x = 28$.

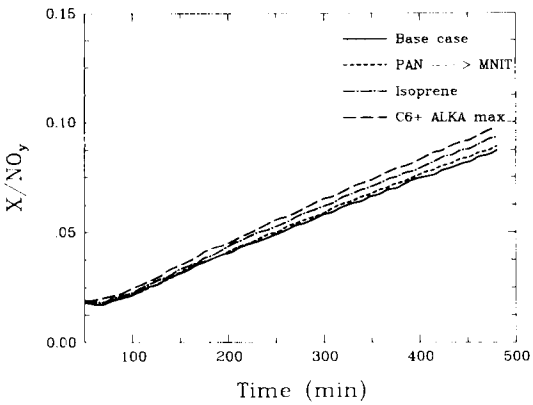

Fig. 6. X/NO_y as a function of time for four scenarios: the base case, a case including the unimolecular decomposition of PAN to form methyl nitrate, a case including an isoprene mechanism, and a case modeling an air parcel containing only $C \geq 6$ alkanes. $HC/NO_x = 7$.

The other two scenarios, the unimolecular decomposition of PAN to form methyl nitrate, and organic nitrate formation from the reactions of isoprene, resulted in changes of less than 0.01 in the quantity X/NO_y.

It is interesting to examine the alkyl nitrate fraction of the quantity X/NO_y for the base case. Alkyl nitrates account for 0.3%, 1.8%, and 4.7% of the total reactive odd nitrogen for the HC/NO_x ratios of 2, 7, and 28, respectively. These translate into total alkyl nitrate concentrations of 0.905 ppbv, 3.03 ppbv, and 4.08 ppbv for $HC/NO_x = 2$, 7, and 28. It is feasible that concentrations of organic nitrates initially on the ppbv level could be reduced by a factor of 10–100 through physical processes and dilution with unpolluted air before reaching measurement sites. Also, if alkyl nitrates are produced in an urban setting and are stable enough to be transported to cleaner environments, where the concentrations of other nitrogen species are lower, then these nitrates could comprise a larger fraction of the total reactive nitrogen reservoir.

While our simulations which included isoprene did not significantly alter our predicted X/NO_y, the importance of natural emissions such as isoprene may increase in cleaner atmospheres. The simulations we ran were typical of urban settings. They are important to investigate because much of the NO_x emitted to the atmosphere is derived from fossil fuel combustion and has at some time in its history been associated with environments of high hydrocarbon concentrations such as those expected in urban areas. Once an air parcel reaches a rural setting, however, natural emissions may be a larger fraction of the total hydrocarbon concentrations, and their chemistry may be more critical.

There are several areas in which experimental data would be useful. Much of the organic nitrate rate data has been determined for reactions of NO with non-substituted peroxy radicals derived from alkanes (Atkinson et al., 1982a; Atkinson et al., 1984; Atkinson and Lloyd, 1984). The explicit mechanism currently assumes no organic nitrates are formed from the reaction of NO and OH-substituted alkyl peroxy radicals. In the past, other models have assumed that the organic nitrate yield from this reaction was equal to that of the non-substituted alkyl peroxy radicals (Leone and Seinfeld, 1985; Atkinson et al., 1982b). Likewise, the explicit mechanism assumes that no organic nitrates are formed from reactions of OH-aromatic-O_2 type adducts.

The mechanism also assumes that no organic nitrates are formed from the reactions of NO and OH-butene-O_2 adducts (Carter et al., 1986). Pre-

vious models have assumed the yield of organic nitrates to be 8% from this reaction by analogy to reactions of non-substituted peroxy radicals produced from butane (Leone and Seinfeld, 1985; Atkinson et al., 1982b). Limited data is available. Experiments with propene (Shepson et al., 1985) have shown that the organic nitrate yield from OH-propene-O_2 radicals is not non-zero, but approximately 0.015. For comparison, the yield from NO reacting with propane-O_2 radicals is 0.04 (Atkinson et al., 1982a). There is the possibility that other alkenes may produce radicals which also may form organic nitrates.

Thus, a considerable degree of uncertainty in nitrogen transformation processes in urban and near-urban settings remains. We have shown, however, that with current chemical mechanisms a significant portion of nitrogen oxides may be transformed to organic nitrates, thereby contributing to the reactive nitrogen shortfall (Fahey et al., 1986).

Table 5. *Nitrogen species represented in the chemical reaction mechanisms*

Both NO, NO_2, HNO_3, HONO, HNO_4, N_2O_5, NO_3	
Condensed	Explicit
alkyl nitrate	2-butyl nitrate
	4-heptyl nitrate
	methyl nitrate
nitrophenol	nitrophenol
	dinitrophenol
PAN (= PAN + PAN analogues)	PAN
	PPN
	glyoxal-PAN
	glycolaldehyde-PAN
	benzene-PAN
	toluene-PAN
	m-xylene-PAN
	o-xylene-PAN
	trimethylbenzene-PAN
	benzaldehyde-PAN

6. Comparison of condensed and explicit mechanisms

Table 5 shows the nitrogen compounds specified by the explicit mechanism and a condensed photochemical mechanism (Lurmann et al., 1987). The explicit mechanism specifies PAN and peroxypropionyl nitrate (PPN) as well as eight additional PAN analogues. The condensed mechanism, however, combines all peroxyacyl nitrates (PAN, PPN, and all other PAN analogues) into a single generic "PAN" category. Actual field measurements reported for PAN typically refer only to the species $CH_3C(O)O_2NO_2$ (Singh and Salas, 1983). PAN has traditionally been of greater concern because its concentration is much higher than each of the higher peroxyacyl nitrates on an individual basis. For example, the concentration of PPN is generally 5–10% that of PAN (Fahey et al., 1986; Singh, 1987). If there are enough different species represented by the PAN analogues present, however, or if they react to form significant amounts of other nitrate species, these analogues could represent an appreciable fraction of the nitrogen budget.

Because the PAN concentration predicted by the condensed mechanism is actually the sum of the concentrations of PAN and all PAN analogues, it is inappropriate for examining the quantity $X/NO_y = 1 - [\sum(NO + NO_2 + NO_3^- + PAN + HNO_3)/NO_y]$. Condensing the mechanism, therefore, results in the loss of information about nitrogen compounds.

We conclude that condensed mechanisms should not be used to examine nitrogen oxide transformations or for comparison to measurements without a thorough comparison of the predictions of such a model to those from an explicit model. In this case, in particular, to study X/NO_y with a condensed mechanism in a grid-based model would require development of a condensed model that included a separate treatment for PAN and the PAN analogues.

7. Conclusion

We have performed box model simulations with an explicit chemical reaction mechanism to examine nitrogen oxide transformation in the polluted troposphere. It is necessary to use an explicit chemical mechanism, as information about nitrogen species may be lost in the process of condensing chemical mechanisms. We exam-

ined organic nitrate formation for a variety of HC/NO_x ratios. The quantity X/NO_y, which represents the fraction of nitrogen present as species other than NO_x, HNO_3, NO_3^-, and PAN equaled 0.24, 0.09, and <0.01 for $HC/NO_x = 28$, 7, and 2, respectively. This quantity contains PAN analogues, whose chemistry is still relatively unknown. The fraction of reactive odd nitrogen present as alkyl nitrates for these same HC/NO_x ratios was 4.7%, 1.8%, and 0.3%, respectively. Of course, the alkyl nitrate fractions could be increased significantly if the PAN analogues formed in our base simulations degraded by autodissociation to form alkyl nitrates.

Several scenarios were run to investigate hypotheses about organic nitrate formation. They included adding an isoprene mechanism to model biogenic hydrocarbon emissions, including the autodissociation of PAN to form methyl nitrate, and starting with an initial mixture whose alkanes contained 6 or more carbon atoms. None of these significantly affected the reactive odd nitrogen species formed. There are still many areas of organic nitrate chemistry that need to be investigated experimentally.

8. Acknowledgements

We wish to thank Peter Connell for his careful reading and comments on the manuscript. This work was performed under the auspices of the U.S. Department of Energy under Contract W-7405-Eng-48 to the Lawrence Livermore National Laboratory.

REFERENCES

Atkinson, R., Aschmann, S. M., Carter, W. P. L., Winer, A. M. and Pitts, J. N. Jr. 1982a. Alkyl nitrate formation from the NO_x-air photooxidations of C_2 – C_8 *n*-alkanes. *J. Phys. Chem. 86*, 4563–4569.

Atkinson, R., Lloyd, A. C. and Winges, L. 1982b. An updated chemical mechanism for hydrocarbon/NO_x/SO_2 photooxidations suitable for inclusion in atmospheric simulation models. *Atmos. Environ. 16*, 1341–1355.

Atkinson, R., Carter, W. P. L. and Winer, A. M. 1983. Effects of temperature and pressure on alkyl nitrate yields in the NO_x photooxidations of *n*-pentane and *n*-heptane. *J. Phys. Chem. 87*, 2012–2018.

Atkinson, R. and Lloyd, A. C. 1984. Evaluation of kinetic and mechanistic data for modeling of photochemical smog. *J. Phys. Chem. Ref. Data 13*, 315–444.

Atkinson, R., Aschmann, S. M., Carter, W. P. L., Winer, A. M. and Pitts, J. N., Jr. 1984. Formation of alkyl nitrates from the reaction of branched and cyclic alkyl peroxy radicals with NO. *Int. J. Chem. Kinet. 16*, 1085–1101.

Atkinson, R., Aschmann, S. M. and Winer, A. M. 1987. Alkyl nitrate formation from the reaction of a series of branched RO_2 radicals with NO as a function of temperature and pressure *J. Atmos. Chem. 5*, 91–102.

Calvert, J. G. and Madronich, S. 1987. Theoretical study of the initial products of the atmospheric oxidation of hydrocarbons. *J. Geophys. Res. 92*, 2211–2220.

Carter, W. P. L., Lurmann, F. W., Atkinson, R. and Lloyd, A. C. 1986. *Development and testing of a surrogate species chemical reaction mechanism, vol. 1.* Report EPA-600/3-86-0031a, U.S. Environ. Prot. Agency, Research Triangle Park, North Carolina, U.S.A.

Cox, R. A. and Tyndall, G. S. 1979. Rate constants for the reactions of CH_3O_2 in the gas phase. *Chem. Phys. Lett. 65*, 357–360.

Darnall, K. R., Carter, W. P. L., Winer, A. M., Lloyd, A. C. and Pitts, J. N., Jr. 1976. Importance of $RO_2 + NO$ in alkyl nitrate formation from $C_4 - C_6$ alkane photooxidations under simulated atmospheric conditions. *J. Phys. Chem. 80*, 1948–1950.

Fahey, D. W., Hubler, G., Parrish, D. D., Williams, E. J., Norton, R. B., Ridley, B. A., Singh, H. B., Liu, S. C. and Fehsenfeld, F. C. 1986. Reactive nitrogen species in the troposphere: measurements of NO, NO_2, HNO_3, particulate nitrate, peroxyacetyl nitrate (PAN), O_3, and total reactive odd nitrogen (NO_y) at Niwot Ridge, Colorado. *J. Geophys. Res. 91*, 9781–9793.

Gaffney, J. S., Fajer, R., Senum, G. I. and Lee, J. H. 1986. Measurement of the reactivity of OH with methyl nitrate: implications for prediction of alkyl nitrate-OH reaction rates. *Int. J. Chem. Kinet. 18*, 399–407.

Gery, M. W., Fox, D. L., Kamens, R. M. and Stockburger, L. 1987. Investigation of hydroxyl radical reactions with *o*-xylene and *m*-xylene in a continuous stirred tank reactor. *Environ. Sci. Technol. 21*, 339–348.

Grosjean, D. and Fung, K. 1984. Hydrocarbons and carbonyls in Los Angeles air. *J. Air Pollut. Control. Assoc. 34*, 537–543.

Hoshino, M., Akimoto, H. and Okuda, M. 1978. Photochemical oxidation of benzene, toluene, and ethylbenzene initiated by OH radicals in the gas phase. *Bull Chem. Soc. Japan 51*, 718–724.

Hov, O. 1984. Modelling of the long-range transport of peroxyacetylnitrate to Scandinavia. *J. Atmos. Chem. 1*, 187–202.

Koppe, R. 1981. *Ambient hydrocarbon concentration field sampling and analysis program.* Report 81/13-22, Bay Area Air Quality Management District, San Francisco, California, U.S.A.

Leone, J. A. and Seinfeld, J. H. 1985. Comparative analysis of chemical reaction mechanisms for photochemical smog. *Atmos. Environ. 19*, 437–464.

Lloyd, A. C., Atkinson, R., Lurmann, F. W. and Nitta, B. 1983. Modeling potential ozone impacts from natural hydrocarbons—I. Development and testing of a chemical mechanism for the NO_x-air photooxidations of isoprene and alpha-pinene under ambient conditions. *Atmos. Environ. 17*, 1931–1950.

Logan, J. A. 1983. Nitrogen oxides in the troposphere: global and regional budgets. *J. Geophys. Res. 88*, 10785–10807.

Lurmann, F. W., Carter, W. P. L. and Coyner, L. A. 1987. *A surrogate species chemical reaction mechanism for urban-scale air quality simulation models, Vol. 1.* Report EPA-600/3-87-041a, U.S. Environ. Prot. Agency, Research Triangle Park, North Carolina, U.S.A.

Parrish, D. D., Williams, E. J., Buhr, M. P., Norton, R. B., Fehsenfeld, F. C., Gandrud, B. W., Ridley, B. A., and Shetter, J. D. 1986. Partitioning of odd-nitrogen species at a rural eastern US site. *EOS 67*, 891.

Penner, J. E. 1984. Modeling the effect of biogenic hydrocarbon emissions in the San Francisco Bay Area. *Proceedings of the APCA Specialty Meeting on the Environmental Impact of Natural Emissions*, March 7–9, 1984, Research Triangle Park, North Carolina, U.S.A.

Penner, J. E. and Connell, P. S. 1987. *Pollutant transport study: Bay Area to North Central Coast Air Basin.* Lawrence Livermore National Laboratory Report UCID-21287, Lawrence Livermore National Laboratory, University of California, Livermore, California, U.S.A.

Rudolph, J. and Khedim, A. 1985. Hydrocarbons in the non-urban atmosphere: analysis, ambient concentrations and impact on the chemistry of the atmosphere. *Intern. J. Environ. Anal. Chem 20*, 265–282.

Senum, G. I., Fajer, R. and Gaffney, J. S. 1986. Fourier transform infrared spectroscopic study of the thermal stability of peroxyacetyl nitrate. *J. Phys. Chem. 90*, 152–156.

Sexton, K. and Westberg, H. 1984. Nonmethane hydrocarbon composition of urban and rural atmospheres, *Atmos. Environ. 18*, 1125–1132.

Shepson, P. B., Edney, E. O., Kleindienst, T. E., Pittman, J. H., Namie, G. R. and Cupitt, L. T. 1985. The production of organic nitrates from hydroxyl and nitrate radical reaction with propylene. *Environ. Sci. Technol. 19*, 849–854.

Singh, H. B. and Salas, L. J. 1983. Methodology for the analysis of peroxyacetyl nitrate (PAN) in the unpolluted atmosphere. *Atmos. Environ. 17*, 1507–1516.

Singh, H. B. 1987. Reactive nitrogen in the troposphere. *Environ. Sci. Technol. 21*, 320–327.

Stephens, E. R. 1969. The formation, reactions, and properties of peroxyacyl nitrates (PANs) in photochemical air pollution. In *Advances in environmental sciences, vol. 1* (eds. J. N. Pitts, Jr. and R. L. Metcalf). New York: John Wiley & Sons, 119–145.

Takagi, H., Washida, N., Bandow, H., Akimoto, H. and Okuda, M. 1981. Photooxidation of C5–C7 cycloalkanes in the NO-H_2O-air system. *J. Phys. Chem. 85*, 2701–2075.

Taylor, W. D., Allston, T. D., Moscato, M. J., Fazekas, G. B., Kozlowski, R. and Takacs, G. A. 1980. Atmospheric photodissociation lifetimes for nitromethane, methyl nitrite, and methyl nitrate. *Int. J. Chem. Kinet. 12*, 231–240.

Tuazon, E. C., MacLeod, H., Atkinson, R. and Carter, W. P. L. 1986. Alpha-dicarbonyl yields from the NO_x-air photooxidations of a series of aromatic hydrocarbons in air. *Environ. Sci. Technol. 20*, 383–387.